

Search for D^0 - \bar{D}^0 Mixing and Branching-Ratio Measurement in the Decay $D^0 \rightarrow K^+\pi^-\pi^0$

B. Aubert,¹ R. Barate,¹ M. Bona,¹ D. Boutigny,¹ F. Couderc,¹ Y. Karyotakis,¹ J. P. Lees,¹ V. Poireau,¹
 V. Tisserand,¹ A. Zghiche,¹ E. Grauges,² A. Palano,³ J. C. Chen,⁴ N. D. Qi,⁴ G. Rong,⁴ P. Wang,⁴ Y. S. Zhu,⁴
 G. Eigen,⁵ I. Ofte,⁵ B. Stugu,⁵ G. S. Abrams,⁶ M. Battaglia,⁶ D. N. Brown,⁶ J. Button-Shafer,⁶ R. N. Cahn,⁶
 E. Charles,⁶ M. S. Gill,⁶ Y. Groysman,⁶ R. G. Jacobsen,⁶ J. A. Kadyk,⁶ L. T. Kerth,⁶ Yu. G. Kolomensky,⁶
 G. Kukartsev,⁶ G. Lynch,⁶ L. M. Mir,⁶ T. J. Orimoto,⁶ M. Pripstein,⁶ N. A. Roe,⁶ M. T. Ronan,⁶ W. A. Wenzel,⁶
 P. del Amo Sanchez,⁷ M. Barrett,⁷ K. E. Ford,⁷ T. J. Harrison,⁷ A. J. Hart,⁷ C. M. Hawkes,⁷ S. E. Morgan,⁷
 A. T. Watson,⁷ T. Held,⁸ H. Koch,⁸ B. Lewandowski,⁸ M. Pelizaeus,⁸ K. Peters,⁸ T. Schroeder,⁸ M. Steinke,⁸
 J. T. Boyd,⁹ J. P. Burke,⁹ W. N. Cottingham,⁹ D. Walker,⁹ T. Cuhadar-Donszelmann,¹⁰ B. G. Fulsom,¹⁰
 C. Hearty,¹⁰ N. S. Knecht,¹⁰ T. S. Mattison,¹⁰ J. A. McKenna,¹⁰ A. Khan,¹¹ P. Kyberd,¹¹ M. Saleem,¹¹
 D. J. Sherwood,¹¹ L. Teodorescu,¹¹ V. E. Blinov,¹² A. D. Bukin,¹² V. P. Druzhinin,¹² V. B. Golubev,¹²
 A. P. Onuchin,¹² S. I. Serednyakov,¹² Yu. I. Skovpen,¹² E. P. Solodov,¹² K. Yu Todyshev,¹² D. S. Best,¹³
 M. Bondioli,¹³ M. Bruinsma,¹³ M. Chao,¹³ S. Curry,¹³ I. Eschrich,¹³ D. Kirkby,¹³ A. J. Lankford,¹³ P. Lund,¹³
 M. Mandelkern,¹³ R. K. Mommsen,¹³ W. Roethel,¹³ D. P. Stoker,¹³ S. Abachi,¹⁴ C. Buchanan,¹⁴ S. D. Foulkes,¹⁵
 J. W. Gary,¹⁵ O. Long,¹⁵ B. C. Shen,¹⁵ K. Wang,¹⁵ L. Zhang,¹⁵ H. K. Hadavand,¹⁶ E. J. Hill,¹⁶ H. P. Paar,¹⁶
 S. Rahatlou,¹⁶ V. Sharma,¹⁶ J. W. Berryhill,¹⁷ C. Campagnari,¹⁷ A. Cunha,¹⁷ B. Dahmes,¹⁷ T. M. Hong,¹⁷
 D. Kovalskyi,¹⁷ J. D. Richman,¹⁷ T. W. Beck,¹⁸ A. M. Eisner,¹⁸ C. J. Flacco,¹⁸ C. A. Heusch,¹⁸ J. Kroeseberg,¹⁸
 W. S. Lockman,¹⁸ G. Nesom,¹⁸ T. Schalk,¹⁸ B. A. Schumm,¹⁸ A. Seiden,¹⁸ P. Spradlin,¹⁸ D. C. Williams,¹⁸
 M. G. Wilson,¹⁸ J. Albert,¹⁹ E. Chen,¹⁹ A. Dvoretskii,¹⁹ F. Fang,¹⁹ D. G. Hitlin,¹⁹ I. Narsky,¹⁹ T. Piatenko,¹⁹
 F. C. Porter,¹⁹ A. Ryd,¹⁹ A. Samuel,¹⁹ G. Mancinelli,²⁰ B. T. Meadows,²⁰ K. Mishra,²⁰ M. D. Sokoloff,²⁰ F. Blanc,²¹
 P. C. Bloom,²¹ S. Chen,²¹ W. T. Ford,²¹ J. F. Hirschauer,²¹ A. Kreisel,²¹ M. Nagel,²¹ U. Nauenberg,²¹ A. Olivas,²¹
 W. O. Ruddick,²¹ J. G. Smith,²¹ K. A. Ulmer,²¹ S. R. Wagner,²¹ J. Zhang,²¹ A. Chen,²² E. A. Eckhart,²²
 A. Soffer,²² W. H. Toki,²² R. J. Wilson,²² F. Winkelmeier,²² Q. Zeng,²² D. D. Altenburg,²³ E. Feltresi,²³ A. Hauke,²³
 H. Jasper,²³ A. Petzold,²³ B. Spaan,²³ T. Brandt,²⁴ V. Klose,²⁴ H. M. Lacker,²⁴ W. F. Mader,²⁴ R. Nogowski,²⁴
 J. Schubert,²⁴ K. R. Schubert,²⁴ R. Schwierz,²⁴ J. E. Sundermann,²⁴ A. Volk,²⁴ D. Bernard,²⁵ G. R. Bonneaud,²⁵
 P. Grenier,²⁵, * E. Latour,²⁵ Ch. Thiebaux,²⁵ M. Verderi,²⁵ P. J. Clark,²⁶ W. Gradl,²⁶ F. Muheim,²⁶ S. Playfer,²⁶
 A. I. Robertson,²⁶ Y. Xie,²⁶ M. Andreotti,²⁷ D. Bettoni,²⁷ C. Bozzi,²⁷ R. Calabrese,²⁷ G. Cibinetto,²⁷ E. Luppi,²⁷
 M. Negrini,²⁷ A. Petrella,²⁷ L. Piemontese,²⁷ E. Prencipe,²⁷ F. Anulli,²⁸ R. Baldini-Ferroli,²⁸ A. Calcaterra,²⁸
 R. de Sangro,²⁸ G. Finocchiaro,²⁸ S. Pacetti,²⁸ P. Patteri,²⁸ I. M. Peruzzi,²⁸, † M. Piccolo,²⁸ M. Rama,²⁸
 A. Zallo,²⁸ A. Buzzo,²⁹ R. Capra,²⁹ R. Contri,²⁹ M. Lo Vetere,²⁹ M. M. Macri,²⁹ M. R. Monge,²⁹ S. Passaggio,²⁹
 C. Patrignani,²⁹ E. Robutti,²⁹ A. Santroni,²⁹ S. Tosi,²⁹ G. Brandenburg,³⁰ K. S. Chaisanguanthum,³⁰ M. Morii,³⁰
 J. Wu,³⁰ R. S. Dubitzky,³¹ J. Marks,³¹ S. Schenk,³¹ U. Uwer,³¹ D. J. Bard,³² W. Bhimji,³² D. A. Bowerman,³²
 P. D. Dauncey,³² U. Egede,³² R. L. Flack,³² J. A. Nash,³² M. B. Nikolich,³² W. Panduro Vazquez,³² P. K. Behera,³³
 X. Chai,³³ M. J. Charles,³³ U. Mallik,³³ N. T. Meyer,³³ V. Ziegler,³³ J. Cochran,³⁴ H. B. Crawley,³⁴ L. Dong,³⁴
 V. Egyes,³⁴ W. T. Meyer,³⁴ S. Prell,³⁴ E. I. Rosenberg,³⁴ A. E. Rubin,³⁴ A. V. Gritsan,³⁵ A. G. Denig,³⁶
 M. Fritsch,³⁶ G. Schott,³⁶ N. Arnaud,³⁷ M. Davier,³⁷ G. Grosdidier,³⁷ A. Höcker,³⁷ F. Le Diberder,³⁷ V. Lepeltier,³⁷
 A. M. Lutz,³⁷ A. Oyanguren,³⁷ S. Pruvot,³⁷ S. Rodier,³⁷ P. Roudeau,³⁷ M. H. Schune,³⁷ A. Stocchi,³⁷
 W. F. Wang,³⁷ G. Wormser,³⁷ C. H. Cheng,³⁸ D. J. Lange,³⁸ D. M. Wright,³⁸ C. A. Chavez,³⁹ I. J. Forster,³⁹
 J. R. Fry,³⁹ E. Gabathuler,³⁹ R. Gamet,³⁹ K. A. George,³⁹ D. E. Hutchcroft,³⁹ D. J. Payne,³⁹ K. C. Schofield,³⁹
 C. Touramanis,³⁹ A. J. Bevan,⁴⁰ F. Di Lodovico,⁴⁰ W. Menges,⁴⁰ R. Sacco,⁴⁰ G. Cowan,⁴¹ H. U. Flaecher,⁴¹
 D. A. Hopkins,⁴¹ P. S. Jackson,⁴¹ T. R. McMahon,⁴¹ S. Ricciardi,⁴¹ F. Salvatore,⁴¹ A. C. Wren,⁴¹ D. N. Brown,⁴²
 C. L. Davis,⁴² J. Allison,⁴³ N. R. Barlow,⁴³ R. J. Barlow,⁴³ Y. M. Chia,⁴³ C. L. Edgar,⁴³ G. D. Lafferty,⁴³
 M. T. Naisbit,⁴³ J. C. Williams,⁴³ J. I. Yi,⁴³ C. Chen,⁴⁴ W. D. Hulsbergen,⁴⁴ A. Jawahery,⁴⁴ C. K. Lae,⁴⁴
 D. A. Roberts,⁴⁴ G. Simi,⁴⁴ G. Blaylock,⁴⁵ C. Dallapiccola,⁴⁵ S. S. Hertzbach,⁴⁵ X. Li,⁴⁵ T. B. Moore,⁴⁵ S. Saremi,⁴⁵
 H. Staengle,⁴⁵ R. Cowan,⁴⁶ G. Sciolla,⁴⁶ S. J. Sekula,⁴⁶ M. Spitznagel,⁴⁶ F. Taylor,⁴⁶ R. K. Yamamoto,⁴⁶ H. Kim,⁴⁷
 S. E. McLachlin,⁴⁷ P. M. Patel,⁴⁷ S. H. Robertson,⁴⁷ A. Lazzaro,⁴⁸ V. Lombardo,⁴⁸ F. Palombo,⁴⁸ J. M. Bauer,⁴⁹
 L. Cremaldi,⁴⁹ V. Eschenburg,⁴⁹ R. Godang,⁴⁹ R. Kroeger,⁴⁹ D. A. Sanders,⁴⁹ D. J. Summers,⁴⁹ H. W. Zhao,⁴⁹
 S. Brunet,⁵⁰ D. Côté,⁵⁰ M. Simard,⁵⁰ P. Taras,⁵⁰ F. B. Viaud,⁵⁰ H. Nicholson,⁵¹ N. Cavallo,⁵², ‡ G. De Nardo,⁵²
 F. Fabozzi,⁵², ‡ C. Gatto,⁵² L. Lista,⁵² D. Monorchio,⁵² P. Paolucci,⁵² D. Piccolo,⁵² C. Sciacca,⁵² M. Baak,⁵³

Submitted to Physical Review Letters

Work supported in part by the US Department of Energy contract DE-AC02-76SF00515

G. Raven,⁵³ H. L. Snoek,⁵³ C. P. Jessop,⁵⁴ J. M. LoSecco,⁵⁴ T. Allmendinger,⁵⁵ G. Benelli,⁵⁵ K. K. Gan,⁵⁵ K. Honscheid,⁵⁵ D. Hufnagel,⁵⁵ P. D. Jackson,⁵⁵ H. Kagan,⁵⁵ R. Kass,⁵⁵ A. M. Rahimi,⁵⁵ R. Ter-Antonyan,⁵⁵ Q. K. Wong,⁵⁵ N. L. Blount,⁵⁶ J. Brau,⁵⁶ R. Frey,⁵⁶ O. Igonkina,⁵⁶ M. Lu,⁵⁶ R. Rahmat,⁵⁶ N. B. Sinev,⁵⁶ D. Strom,⁵⁶ J. Strube,⁵⁶ E. Torrence,⁵⁶ A. Gaz,⁵⁷ M. Margoni,⁵⁷ M. Morandin,⁵⁷ A. Pompili,⁵⁷ M. Posocco,⁵⁷ M. Rotondo,⁵⁷ F. Simonetto,⁵⁷ R. Stroili,⁵⁷ C. Voci,⁵⁷ M. Benayoun,⁵⁸ J. Chauveau,⁵⁸ H. Briand,⁵⁸ P. David,⁵⁸ L. Del Buono,⁵⁸ Ch. de la Vaissière,⁵⁸ O. Hamon,⁵⁸ B. L. Hartfiel,⁵⁸ M. J. J. John,⁵⁸ Ph. Leruste,⁵⁸ J. Malclès,⁵⁸ J. Ocariz,⁵⁸ L. Roos,⁵⁸ G. Therin,⁵⁸ L. Gladney,⁵⁹ J. Panetta,⁵⁹ M. Biasini,⁶⁰ R. Covarelli,⁶⁰ C. Angelini,⁶¹ G. Batignani,⁶¹ S. Bettarini,⁶¹ F. Bucci,⁶¹ G. Calderini,⁶¹ M. Carpinelli,⁶¹ R. Cenci,⁶¹ F. Forti,⁶¹ M. A. Giorgi,⁶¹ A. Lusiani,⁶¹ G. Marchiori,⁶¹ M. A. Mazur,⁶¹ M. Morganti,⁶¹ N. Neri,⁶¹ E. Paoloni,⁶¹ G. Rizzo,⁶¹ J. J. Walsh,⁶¹ M. Haire,⁶² D. Judd,⁶² D. E. Wagoner,⁶² J. Biesiada,⁶³ N. Danielson,⁶³ P. Elmer,⁶³ Y. P. Lau,⁶³ C. Lu,⁶³ J. Olsen,⁶³ A. J. S. Smith,⁶³ A. V. Telnov,⁶³ F. Bellini,⁶⁴ G. Cavoto,⁶⁴ A. D'Orazio,⁶⁴ D. del Re,⁶⁴ E. Di Marco,⁶⁴ R. Faccini,⁶⁴ F. Ferrarotto,⁶⁴ F. Ferroni,⁶⁴ M. Gaspero,⁶⁴ L. Li Gioi,⁶⁴ M. A. Mazzoni,⁶⁴ S. Morganti,⁶⁴ G. Piredda,⁶⁴ F. Polci,⁶⁴ F. Safai Tehrani,⁶⁴ C. Voena,⁶⁴ M. Ebert,⁶⁵ H. Schröder,⁶⁵ R. Waldi,⁶⁵ T. Adye,⁶⁶ N. De Groot,⁶⁶ B. Franek,⁶⁶ E. O. Olaiya,⁶⁶ F. F. Wilson,⁶⁶ R. Aleksan,⁶⁷ S. Emery,⁶⁷ A. Gaidot,⁶⁷ S. F. Ganzhur,⁶⁷ G. Hamel de Monchenault,⁶⁷ W. Kozanecki,⁶⁷ M. Legendre,⁶⁷ G. Vasseur,⁶⁷ Ch. Yèche,⁶⁷ M. Zito,⁶⁷ X. R. Chen,⁶⁸ H. Liu,⁶⁸ W. Park,⁶⁸ M. V. Purohit,⁶⁸ J. R. Wilson,⁶⁸ M. T. Allen,⁶⁹ D. Aston,⁶⁹ R. Bartoldus,⁶⁹ P. Bechtle,⁶⁹ N. Berger,⁶⁹ R. Claus,⁶⁹ J. P. Coleman,⁶⁹ M. R. Convery,⁶⁹ M. Cristinziani,⁶⁹ J. C. Dingfelder,⁶⁹ J. Dorfan,⁶⁹ G. P. Dubois-Felsmann,⁶⁹ D. Dujmic,⁶⁹ W. Dunwoodie,⁶⁹ R. C. Field,⁶⁹ T. Glanzman,⁶⁹ S. J. Gowdy,⁶⁹ M. T. Graham,⁶⁹ V. Halyo,⁶⁹ C. Hast,⁶⁹ T. Hryna'ova,⁶⁹ W. R. Innes,⁶⁹ M. H. Kelsey,⁶⁹ P. Kim,⁶⁹ D. W. G. S. Leith,⁶⁹ S. Li,⁶⁹ S. Luitz,⁶⁹ V. Luth,⁶⁹ H. L. Lynch,⁶⁹ D. B. MacFarlane,⁶⁹ H. Marsiske,⁶⁹ R. Messner,⁶⁹ D. R. Muller,⁶⁹ C. P. O'Grady,⁶⁹ V. E. Ozcan,⁶⁹ A. Perazzo,⁶⁹ M. Perl,⁶⁹ T. Pulliam,⁶⁹ B. N. Ratcliff,⁶⁹ A. Roodman,⁶⁹ A. A. Salnikov,⁶⁹ R. H. Schindler,⁶⁹ J. Schwiening,⁶⁹ A. Snyder,⁶⁹ J. Stelzer,⁶⁹ D. Su,⁶⁹ M. K. Sullivan,⁶⁹ K. Suzuki,⁶⁹ S. K. Swain,⁶⁹ J. M. Thompson,⁶⁹ J. Va'vra,⁶⁹ N. van Bakel,⁶⁹ M. Weaver,⁶⁹ A. J. R. Weinstein,⁶⁹ W. J. Wisniewski,⁶⁹ M. Wittgen,⁶⁹ D. H. Wright,⁶⁹ A. K. Yarritu,⁶⁹ K. Yi,⁶⁹ C. C. Young,⁶⁹ P. R. Burchat,⁷⁰ A. J. Edwards,⁷⁰ S. A. Majewski,⁷⁰ B. A. Petersen,⁷⁰ C. Roat,⁷⁰ L. Wilden,⁷⁰ S. Ahmed,⁷¹ M. S. Alam,⁷¹ R. Bula,⁷¹ J. A. Ernst,⁷¹ V. Jain,⁷¹ B. Pan,⁷¹ M. A. Saeed,⁷¹ F. R. Wappler,⁷¹ S. B. Zain,⁷¹ W. Bugg,⁷² M. Krishnamurthy,⁷² S. M. Spanier,⁷² R. Eckmann,⁷³ J. L. Ritchie,⁷³ A. Satpathy,⁷³ C. J. Schilling,⁷³ R. F. Schwitters,⁷³ J. M. Izen,⁷⁴ X. C. Lou,⁷⁴ S. Ye,⁷⁴ F. Bianchi,⁷⁵ F. Gallo,⁷⁵ D. Gamba,⁷⁵ M. Bomben,⁷⁶ L. Bosisio,⁷⁶ C. Cartaro,⁷⁶ F. Cossutti,⁷⁶ G. Della Ricca,⁷⁶ S. Dittongo,⁷⁶ L. Lanceri,⁷⁶ L. Vitale,⁷⁶ V. Azzolini,⁷⁷ F. Martinez-Vidal,⁷⁷ Sw. Banerjee,⁷⁸ B. Bhuyan,⁷⁸ C. M. Brown,⁷⁸ D. Fortin,⁷⁸ K. Hamano,⁷⁸ R. Kowalewski,⁷⁸ I. M. Nugent,⁷⁸ J. M. Roney,⁷⁸ R. J. Sobie,⁷⁸ J. J. Back,⁷⁹ P. F. Harrison,⁷⁹ T. E. Latham,⁷⁹ G. B. Mohanty,⁷⁹ M. Pappagallo,⁷⁹ H. R. Band,⁸⁰ X. Chen,⁸⁰ B. Cheng,⁸⁰ S. Dasu,⁸⁰ M. Datta,⁸⁰ K. T. Flood,⁸⁰ J. J. Hollar,⁸⁰ P. E. Kutter,⁸⁰ B. Mellado,⁸⁰ A. Mihalyi,⁸⁰ Y. Pan,⁸⁰ M. Pierini,⁸⁰ R. Prepost,⁸⁰ S. L. Wu,⁸⁰ Z. Yu,⁸⁰ and H. Neal⁸¹

(The BABAR Collaboration)

¹Laboratoire de Physique des Particules, F-74941 Annecy-le-Vieux, France

²Universitat de Barcelona, Facultat de Fisica, Departament ECM, E-08028 Barcelona, Spain

³Università di Bari, Dipartimento di Fisica and INFN, I-70126 Bari, Italy

⁴Institute of High Energy Physics, Beijing 100039, China

⁵University of Bergen, Institute of Physics, N-5007 Bergen, Norway

⁶Lawrence Berkeley National Laboratory and University of California, Berkeley, California 94720, USA

⁷University of Birmingham, Birmingham, B15 2TT, United Kingdom

⁸Ruhr Universität Bochum, Institut für Experimentalphysik 1, D-44780 Bochum, Germany

⁹University of Bristol, Bristol BS8 1TL, United Kingdom

¹⁰University of British Columbia, Vancouver, British Columbia, Canada V6T 1Z1

¹¹Brunel University, Uxbridge, Middlesex UB8 3PH, United Kingdom

¹²Budker Institute of Nuclear Physics, Novosibirsk 630090, Russia

¹³University of California at Irvine, Irvine, California 92697, USA

¹⁴University of California at Los Angeles, Los Angeles, California 90024, USA

¹⁵University of California at Riverside, Riverside, California 92521, USA

¹⁶University of California at San Diego, La Jolla, California 92093, USA

¹⁷University of California at Santa Barbara, Santa Barbara, California 93106, USA

¹⁸University of California at Santa Cruz, Institute for Particle Physics, Santa Cruz, California 95064, USA

¹⁹California Institute of Technology, Pasadena, California 91125, USA

²⁰University of Cincinnati, Cincinnati, Ohio 45221, USA

²¹University of Colorado, Boulder, Colorado 80309, USA

- ²²Colorado State University, Fort Collins, Colorado 80523, USA
²³Universität Dortmund, Institut für Physik, D-44221 Dortmund, Germany
²⁴Technische Universität Dresden, Institut für Kern- und Teilchenphysik, D-01062 Dresden, Germany
²⁵Ecole Polytechnique, Laboratoire Leprince-Ringuet, F-91128 Palaiseau, France
²⁶University of Edinburgh, Edinburgh EH9 3JZ, United Kingdom
²⁷Università di Ferrara, Dipartimento di Fisica and INFN, I-44100 Ferrara, Italy
²⁸Laboratori Nazionali di Frascati dell'INFN, I-00044 Frascati, Italy
²⁹Università di Genova, Dipartimento di Fisica and INFN, I-16146 Genova, Italy
³⁰Harvard University, Cambridge, Massachusetts 02138, USA
³¹Universität Heidelberg, Physikalisches Institut, Philosophenweg 12, D-69120 Heidelberg, Germany
³²Imperial College London, London, SW7 2AZ, United Kingdom
³³University of Iowa, Iowa City, Iowa 52242, USA
³⁴Iowa State University, Ames, Iowa 50011-3160, USA
³⁵Johns Hopkins University, Baltimore, Maryland 21218, USA
³⁶Universität Karlsruhe, Institut für Experimentelle Kernphysik, D-76021 Karlsruhe, Germany
³⁷Laboratoire de l'Accélérateur Linéaire, IN2P3-CNRS et Université Paris-Sud 11, Centre Scientifique d'Orsay, B.P. 34, F-91898 ORSAY Cedex, France
³⁸Lawrence Livermore National Laboratory, Livermore, California 94550, USA
³⁹University of Liverpool, Liverpool L69 7ZE, United Kingdom
⁴⁰Queen Mary, University of London, E1 4NS, United Kingdom
⁴¹University of London, Royal Holloway and Bedford New College, Egham, Surrey TW20 0EX, United Kingdom
⁴²University of Louisville, Louisville, Kentucky 40292, USA
⁴³University of Manchester, Manchester M13 9PL, United Kingdom
⁴⁴University of Maryland, College Park, Maryland 20742, USA
⁴⁵University of Massachusetts, Amherst, Massachusetts 01003, USA
⁴⁶Massachusetts Institute of Technology, Laboratory for Nuclear Science, Cambridge, Massachusetts 02139, USA
⁴⁷McGill University, Montréal, Québec, Canada H3A 2T8
⁴⁸Università di Milano, Dipartimento di Fisica and INFN, I-20133 Milano, Italy
⁴⁹University of Mississippi, University, Mississippi 38677, USA
⁵⁰Université de Montréal, Physique des Particules, Montréal, Québec, Canada H3C 3J7
⁵¹Mount Holyoke College, South Hadley, Massachusetts 01075, USA
⁵²Università di Napoli Federico II, Dipartimento di Scienze Fisiche and INFN, I-80126, Napoli, Italy
⁵³NIKHEF, National Institute for Nuclear Physics and High Energy Physics, NL-1009 DB Amsterdam, The Netherlands
⁵⁴University of Notre Dame, Notre Dame, Indiana 46556, USA
⁵⁵Ohio State University, Columbus, Ohio 43210, USA
⁵⁶University of Oregon, Eugene, Oregon 97403, USA
⁵⁷Università di Padova, Dipartimento di Fisica and INFN, I-35131 Padova, Italy
⁵⁸Universités Paris VI et VII, Laboratoire de Physique Nucléaire et de Hautes Energies, F-75252 Paris, France
⁵⁹University of Pennsylvania, Philadelphia, Pennsylvania 19104, USA
⁶⁰Università di Perugia, Dipartimento di Fisica and INFN, I-06100 Perugia, Italy
⁶¹Università di Pisa, Dipartimento di Fisica, Scuola Normale Superiore and INFN, I-56127 Pisa, Italy
⁶²Prairie View A&M University, Prairie View, Texas 77446, USA
⁶³Princeton University, Princeton, New Jersey 08544, USA
⁶⁴Università di Roma La Sapienza, Dipartimento di Fisica and INFN, I-00185 Roma, Italy
⁶⁵Universität Rostock, D-18051 Rostock, Germany
⁶⁶Rutherford Appleton Laboratory, Chilton, Didcot, Oxon, OX11 0QX, United Kingdom
⁶⁷DSM/Dapnia, CEA/Saclay, F-91191 Gif-sur-Yvette, France
⁶⁸University of South Carolina, Columbia, South Carolina 29208, USA
⁶⁹Stanford Linear Accelerator Center, Stanford, California 94309, USA
⁷⁰Stanford University, Stanford, California 94305-4060, USA
⁷¹State University of New York, Albany, New York 12222, USA
⁷²University of Tennessee, Knoxville, Tennessee 37996, USA
⁷³University of Texas at Austin, Austin, Texas 78712, USA
⁷⁴University of Texas at Dallas, Richardson, Texas 75083, USA
⁷⁵Università di Torino, Dipartimento di Fisica Sperimentale and INFN, I-10125 Torino, Italy
⁷⁶Università di Trieste, Dipartimento di Fisica and INFN, I-34127 Trieste, Italy
⁷⁷IFIC, Universitat de Valencia-CSIC, E-46071 Valencia, Spain
⁷⁸University of Victoria, Victoria, British Columbia, Canada V8W 3P6
⁷⁹Department of Physics, University of Warwick, Coventry CV4 7AL, United Kingdom
⁸⁰University of Wisconsin, Madison, Wisconsin 53706, USA
⁸¹Yale University, New Haven, Connecticut 06511, USA

(Dated: January 5, 2007)

We analyze 230.4 fb^{-1} of data collected with the *BABAR* detector at the PEP-II e^+e^- collider at SLAC to search for evidence of $D^0-\bar{D}^0$ mixing using regions of phase space in the decay $D^0 \rightarrow K^+\pi^-\pi^0$. We measure the time-integrated mixing rate $R_M = (0.023^{+0.018}_{-0.014} \text{ (stat.)} \pm 0.004 \text{ (syst.)})\%$, and $R_M < 0.054\%$ at the 95% confidence level, assuming CP invariance. The data are consistent with no mixing at the 4.5% confidence level. We also measure the branching ratio for $D^0 \rightarrow K^+\pi^-\pi^0$ relative to $D^0 \rightarrow K^-\pi^+\pi^0$ to be $(0.214 \pm 0.008 \text{ (stat.)} \pm 0.008 \text{ (syst.)})\%$.

PACS numbers: 14.40.Lb, 13.25.Ft, 12.15.Mm, 11.30.Er

Mixing of the strong eigenstates $|D^0\rangle$ and $|\bar{D}^0\rangle$, involving transitions of the charm quark to a down-type quark, is expected to have a very small rate in the Standard Model (SM). Accurate estimates of this rate must consider long-distance effects [1], and typical theoretical values of the time-integrated mixing rate are $R_M \sim \mathcal{O}(10^{-6}\text{--}10^{-4})$. The most stringent constraint to date is $R_M < 0.040\%$ at the 95% confidence level [2]. Because SM D mixing involves only the first two quark generations to a very good approximation, the mixing-amplitude scale is set by flavor-SU(3) breaking, and CP violation is undetectable [1].

We search for the process $|D^0\rangle \rightarrow |\bar{D}^0\rangle$ by analyzing the decay of a particle known to be created as a $|D^0\rangle$ [3]. We reconstruct the wrong-sign (WS) decay $D^0 \rightarrow K^+\pi^-\pi^0$, and we distinguish doubly Cabibbo-suppressed (DCS) contributions from Cabibbo-favored (CF) mixed contributions in the decay-time distribution. Because mixing amplitudes are small, the greatest sensitivity to mixing is found when the amplitude for a particular DCS decay is comparably small. We increase our overall sensitivity to mixing by selecting regions of phase space (*i.e.*, the Dalitz plot) where the relative number of DCS decays to CF decays is small. This technique cannot be performed with the two-body decay $D^0 \rightarrow K^+\pi^-$, and it has not been used to date. While the ratio of DCS to CF decay rates depends on position in the Dalitz plot, the mixing rate does not. From inspection of the Dalitz plots, we note that DCS decays proceed primarily through the resonance $D^0 \rightarrow K^{*+}\pi^-$, while CF decays proceed primarily through $D^0 \rightarrow K^-\rho^+$ [4].

We present the first search for D mixing in the decay $D^0 \rightarrow K^+\pi^-\pi^0$. The analysis method introduced increases experimental accessibility to interference between DCS decay and mixing without a full phase-space parameterization. Such interference effects can be used to search for new physics contributions to CP violation.

The two mass eigenstates

$$|D_{A,B}\rangle = p|D^0\rangle \pm q|\bar{D}^0\rangle \quad (1)$$

generated by mixing dynamics have different masses ($m_{A,B}$) and widths ($\Gamma_{A,B}$), and we parameterize the mixing process with the quantities

$$x \equiv 2\frac{m_B - m_A}{\Gamma_B + \Gamma_A}, \quad y \equiv \frac{\Gamma_B - \Gamma_A}{\Gamma_B + \Gamma_A}. \quad (2)$$

If CP is not violated, then $|p/q| = 1$. For a nonleptonic multibody WS decay, the time-dependent decay

rate, $\Gamma_{\text{WS}}(t)$, relative to a corresponding right-sign (RS) rate, $\Gamma_{\text{RS}}(t)$, is approximated by [5]

$$\frac{\Gamma_{\text{WS}}(t)}{\Gamma_{\text{RS}}(t)} = \tilde{R}_D + \alpha \tilde{y}' \sqrt{\tilde{R}_D} (\Gamma t) + \frac{\tilde{x}'^2 + \tilde{y}'^2}{4} (\Gamma t)^2 \quad (3)$$

$$0 \leq \alpha \leq 1.$$

The tilde indicates quantities that have been integrated over any choice of phase-space regions. \tilde{R}_D is the integrated DCS branching ratio, $\tilde{y}' = y \cos \tilde{\delta} - x \sin \tilde{\delta}$ and $\tilde{x}' = x \cos \tilde{\delta} + y \sin \tilde{\delta}$, where $\tilde{\delta}$ is an integrated strong-phase difference between the CF and the DCS decay amplitudes, α is a suppression factor that accounts for strong-phase variation over the regions, and Γ is the average width. The time-integrated mixing rate $R_M = (\tilde{x}'^2 + \tilde{y}'^2)/2 = (x^2 + y^2)/2$ is independent of decay mode.

We search for CP -violating effects by fitting to the $D^0 \rightarrow K^+\pi^-\pi^0$ and $\bar{D}^0 \rightarrow K^-\pi^+\pi^0$ samples separately. We consider CP violation in the interference between the DCS channel and mixing, parameterized by an integrated CP -violating-phase difference $\tilde{\phi}$, as well as CP violation in mixing, parameterized by $|p/q|$. We assume CP invariance in the DCS and CF decay rates. The substitutions

$$\alpha \tilde{y}' \rightarrow |p/q|^{\pm 1} (\alpha \tilde{y}' \cos \tilde{\phi} \pm \beta \tilde{x}' \sin \tilde{\phi}) \quad (4)$$

$$(x^2 + y^2) \rightarrow |p/q|^{\pm 2} (x^2 + y^2) \quad (5)$$

are applied to Eq. 3, using (+) for $\Gamma(\bar{D}^0 \rightarrow K^-\pi^+\pi^0)/\Gamma(D^0 \rightarrow K^-\pi^+\pi^0)$ and (-) for the charge-conjugate ratio. The parameter β is a suppression factor that accounts for ϕ variation in the selected regions.

We use 230.4 fb^{-1} of data collected with the *BABAR* detector [6] at the PEP-II e^+e^- collider at SLAC. The production vertices of charged particles are measured with a silicon-strip detector (SVT), and their momenta are measured by the SVT and a drift chamber (DCH) in a 1.5 T magnetic field. Particle types are identified using energy deposition measurements from the SVT and DCH along with information from a Cherenkov-radiation detector. The energies of photons are measured by an electromagnetic calorimeter. All selection criteria were finalized before searching for evidence of mixing in the data. Selection criteria were determined from both study of the RS sample and past experience with other charm samples [7].

We reconstruct the decay $D^{*+} \rightarrow D^0\pi_s^+$ and determine the flavor of the D^0 candidate from the charge of the low-momentum pion denoted by π_s^\pm . We require π_s^\pm

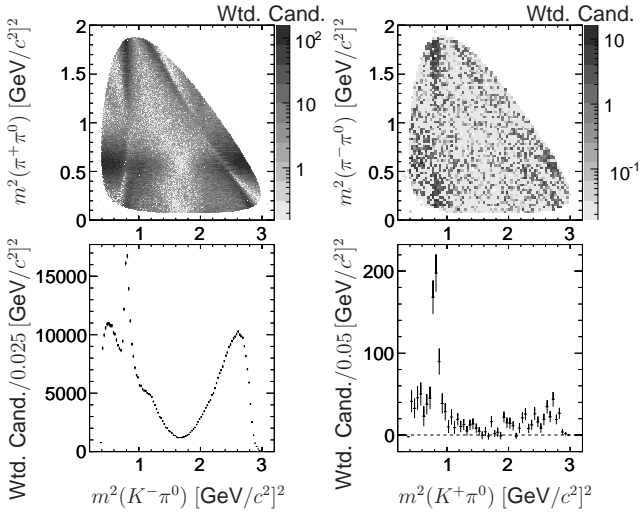


FIG. 1: Dalitz plots and projections for RS (left) and WS (right) data. An additional selection is made to reduce peaking background in the events shown here, and no σ_t selection is made. A statistical background subtraction [11] and a phase-space dependent efficiency correction have been applied (*i.e.*, candidates have been weighted).

candidates to have momentum transverse to the beam axis $p_t > 120 \text{ MeV}/c$. We require D^0 candidates to have center-of-mass momenta greater than $2.4 \text{ GeV}/c$, and the charged D^0 daughters must satisfy a likelihood-based particle-identification selection. The identification efficiency for both K and π is 90%, and the misidentification rate is 3% (1%) for K (π) candidates. We require photons from π^0 decays to have a laboratory energy $E_\gamma > 100 \text{ MeV}$, and π^0 candidates to have a laboratory momentum $p_{\pi^0} > 350 \text{ MeV}/c$ and a mass-constrained-fit χ^2 probability > 0.01 . The experimental width of the π^0 -mass peak is $\sigma_{m(\gamma\gamma)} \approx 6 \text{ MeV}/c^2$. We accept candidates with an invariant mass $1.74 < m_{K\pi\pi^0} < 1.98 \text{ GeV}/c^2$ and an invariant mass difference $0.140 < \Delta m < 0.155 \text{ GeV}/c^2$, where $\Delta m \equiv m_{K\pi\pi^0\pi_s} - m_{K\pi\pi^0}$. We enhance contributions from $D^0 \rightarrow K^- \rho^+$ and reduce the ratio of DCS to CF decays by excluding events with two-body invariant masses in the ranges $850 < m(K\pi^\pm, K\pi^0) < 950 \text{ MeV}/c^2$. Figure 1 shows the Dalitz plots for these decays.

The D^{*+} mass, D^0 mass, and D^0 decay time are derived from a track-vertex fit [8]. A mass constraint is applied to the π^0 candidate, and the D^{*+} -decay vertex is constrained to the beamspot region, of size $(\sigma_x, \sigma_y, \sigma_z) \approx (150 \mu\text{m}, 10 \mu\text{m}, 7 \text{ mm})$. We select events for which the fit χ^2 probability > 0.01 . From this fit, a D^0 decay time, t , and uncertainty, σ_t , are calculated using the three-dimensional flight path. The full covariance matrix, including correlations between the D^{*+} and D^0 vertices, is used in the σ_t estimate. For signal events, the typical value of σ_t is near 0.23 ps. We accept decays with $\sigma_t < 0.5 \text{ ps}$. The D^0 lifetime is $(410.1 \pm 1.5) \text{ fs}$ [9].

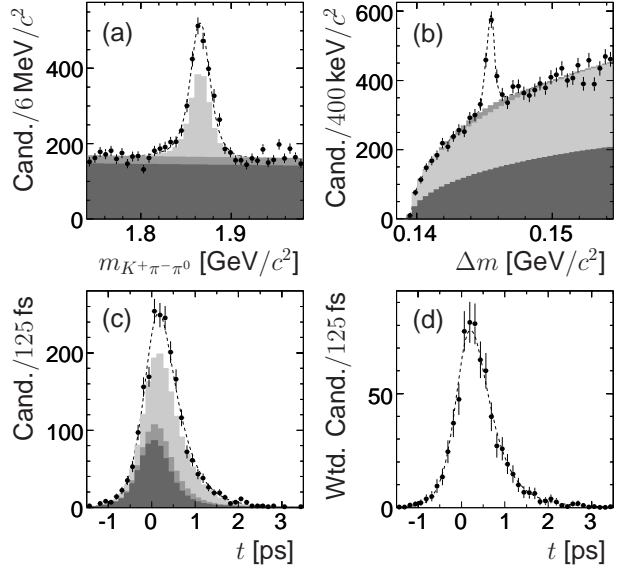


FIG. 2: Distributions of WS data (points with error bars) with fitted PDFs (dashed line) overlaid. The $m_{K\pi\pi^0}$ distribution (a) requires $0.1444 < \Delta m < 0.1464 \text{ GeV}/c^2$; the Δm distribution (b) requires $1.85 < m_{K\pi\pi^0} < 1.88 \text{ GeV}/c^2$; and the t distribution (c) requires both mass selections. The data points in (d) show the t distribution after applying a channel-likelihood signal projection [11, 12], and the signal PDF is overlaid. The error bars in (d) reflect Poissonian signal fluctuations only. In (a)–(d), the white regions represent signal events, the light gray misassociated π_s^\pm events, the medium gray correctly associated π_s^\pm with misreconstructed D^0 events, and the dark gray remaining combinatorial background.

We first extract the signal yields from a two-dimensional, unbinned, extended maximum likelihood fit to the $m_{K\pi\pi^0}$ and Δm distributions, performed on the RS and WS samples simultaneously. The signal-shape parameters of the probability density function (PDF) describing the WS sample are precisely determined by the large RS sample, and all associated systematic uncertainties are suppressed. The width of the Δm peak is uncorrelated with the width of the $m_{K\pi\pi^0}$ peak, dominated by π^0 -momentum resolution, to first order. However, there is a second-order correlation in the signal between the two distributions. Thus, the signal PDF has a width in Δm that varies quadratically with $m_{K\pi\pi^0}$. This feature significantly reduces the signal yield uncertainty.

Three background categories are included in the likelihood: (1) correctly reconstructed D^0 candidates with a misassociated π_s^+ , (2) D^{*+} decays with a correctly associated π_s^+ and a misreconstructed D^0 , and (3) remaining combinatorial backgrounds. The first category has distributions in $m_{K\pi\pi^0}$ and t of RS signal decays and is distinguished using Δm . The second category, peaking in Δm and distinguished using $m_{K\pi\pi^0}$, has a t distribution similar to RS signal with a different characteristic lifetime.

TABLE I: Signal-candidate yields determined by the two-dimensional fit to the $(m_{K\pi\pi^0}, \Delta m)$ distributions for the WS and RS samples. Yields are shown (a) for the selected phase-space regions used in this analysis and (b) for the entire allowed phase-space region. Uncertainties are those calculated from the fit, and no efficiency corrections have been applied.

| | D^0 Cand. | \bar{D}^0 Cand. |
|-----|------------------------------------|---------------------------------|
| (a) | WS $(3.84 \pm 0.36) \times 10^2$ | $(3.79 \pm 0.36) \times 10^2$ |
| | RS $(2.518 \pm 0.006) \times 10^5$ | $(2.512 \pm 0.006) \times 10^5$ |
| (b) | WS $(7.5 \pm 0.5) \times 10^2$ | $(8.1 \pm 0.5) \times 10^2$ |
| | RS $(3.648 \pm 0.007) \times 10^5$ | $(3.646 \pm 0.007) \times 10^5$ |

The third category does not peak in either $m_{K\pi\pi^0}$ or Δm and has a t distribution empirically described by a Gaussian with a power-law tail. Although the functional forms of the background PDFs are motivated by simulations, all shape parameters are obtained from a fit to the data. The $m_{K\pi\pi^0}$ and Δm projections of the two-dimensional fit to the WS sample are shown in Fig. 2(a,b).

The signal yields from the fit to the $(m_{K\pi\pi^0}, \Delta m)$ plane are listed in Table I. Considering the entire allowed phase space, and without the σ_t selection, we measure the branching ratio for $D^0 \rightarrow K^+\pi^-\pi^0$ relative to the decay $D^0 \rightarrow K^-\pi^+\pi^0$ to be $(0.214 \pm 0.008\text{(stat.)} \pm 0.008\text{(syst.)})\%$. This result is consistent with previous measurements [10] of this quantity and is significantly more precise. For this measurement, a phase-space dependent efficiency correction is applied to account for the different resonant populations in CF and DCS decays. The average efficiency of the WS sample relative to the RS samples is 97%. Phase-space dependent π^0 selection efficiencies dominate the systematic uncertainty.

The fitted shape parameters from $m_{K\pi\pi^0}$ and Δm are used to determine the signal probability of each event in a three-dimensional likelihood, \mathcal{L} , that is optimized in a one-dimensional fit to t . The RS signal PDF in t is represented by an exponential function convolved with a three-Gaussian detector-resolution function. The Gaussians have a common mean, but different widths. The width of each Gaussian is a scale factor multiplied by σ_t , and σ_t is determined for each event. The three different scale factors, as well as the fraction of events described by each Gaussian, are determined from the fit to the data. We find a D^0 lifetime consistent with the nominal value.

The WS PDF in t is based on Eq. 3 convolved with the same resolution function as in the RS PDF. The D^0 lifetime and resolution scale factors, determined by the fit to the RS t distribution, are fixed. We fit the WS PDF to the t distribution allowing yields and background-shape parameters to vary. The fit to the t distribution is shown for the WS sample in Fig. 2(c,d).

The results of the decay-time fit, with and without the assumption of CP conservation, are listed in Ta-

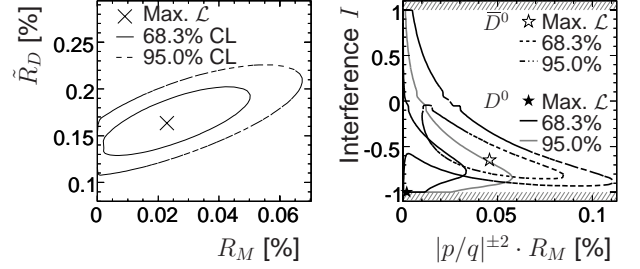


FIG. 3: Contours of constant $\Delta \ln \mathcal{L} = 1.15, 3$, defining 68.3% and 95.0% confidence levels, respectively. The contours on the left are in terms of the integrated mixing rate, R_M , and doubly Cabibbo-suppressed rate, \tilde{R}_D , assuming CP invariance. The contours on the right are in terms of R_M and the normalized interference $I = (\alpha \tilde{x}' \cos \tilde{\phi} \pm \beta \tilde{x}' \sin \tilde{\phi}) / \sqrt{x^2 + y^2}$, for the D^0 and \bar{D}^0 samples separately. On the left, the upward slope of the contour indicates negative interference; on the right, the hatched regions are physically forbidden.

ble II. The statistical uncertainty of a particular parameter is obtained by finding its extrema for $\Delta \ln \mathcal{L} = 0.5$. Contours of constant $\Delta \ln \mathcal{L} = 1.15, 3$, enclosing two-dimensional coverage probabilities of 68.3% and 95.0%, respectively, are shown in Fig. 3. With a Bayesian interpretation of \mathcal{L} , we find an upper limit $R_M < 0.054\%$ at the 95% confidence level, assuming CP conservation.

In one dimension, $\Delta \ln \mathcal{L}$ changes its behavior near $R_M = 0$ because the interference term (the term linear in t in Eq. 3) becomes unconstrained. Therefore, we estimate the consistency of the data with no mixing using a frequentist method. We generate 1000 simulated data sets with no mixing but otherwise according to the fitted PDF, each with 58,800 events representing signal and background in the quantities $m_{K\pi\pi^0}$, Δm , and t . We find 4.5% of simulated data sets have a fitted value of R_M greater than that observed in the data. Thus, the observed data are consistent with no mixing at the 4.5% confidence level.

We quantify systematic uncertainties by repeating the fits with the following elements changed, in order of significance: the background PDF shape in the $m_{K\pi\pi^0}$ distribution, the selection of events based on σ_t , the decay-time resolution function, and the measured D^0 lifetime value. Additionally, for \tilde{R}_D , we consider the absence of any Dalitz-plot efficiency correction. The combined systematic uncertainties are smaller than statistical uncertainties by factors of 2–4. The quantity $\beta \tilde{x}' \sin \tilde{\phi}$, which quantifies a difference between the D^0 and \bar{D}^0 samples, has a negligible systematic uncertainty because positively correlated effects in the two samples cancel.

As a consistency check, we perform the decay-time fit to the entire phase-space region populated by the decays $D^0 \rightarrow K^+\pi^-\pi^0$. The results are consistent with Table II, with sensitivity to R_M preserved. However, the interference term obtained is different. Figure 3 indicates that

TABLE II: Mixing results assuming CP conservation (D^0 and \bar{D}^0 samples are not separated) and manifestly permitting CP violation (D^0 and \bar{D}^0 samples are fit separately). The first listed uncertainty is statistical, and the second is systematic. Quantities that have been integrated over the selected phase-space regions are indicated with tildes. \tilde{R}_D is not reported when allowing for CP violation because precise π_s^\pm efficiency asymmetries are unknown.

| CP conserved | | CP violation allowed |
|--------------------|---|---|
| R_M | $(0.023^{+0.018}_{-0.014} \pm 0.004)\%$ | $(0.010^{+0.022}_{-0.007} \pm 0.003)\%$ |
| \tilde{R}_D | $(0.164^{+0.026}_{-0.022} \pm 0.012)\%$ | |
| | | $\alpha\tilde{y}' \cos\tilde{\phi}$ |
| $\alpha\tilde{y}'$ | $-0.012^{+0.006}_{-0.008} \pm 0.002$ | $-0.012^{+0.006}_{-0.007} \pm 0.002$ |
| | | $\beta\tilde{x}' \sin\tilde{\phi}$ |
| | | $0.003^{+0.002}_{-0.005} \pm 0.000$ |
| | | $ p/q $ |
| | | $2.2^{+1.9}_{-1.0} \pm 0.1$ |

both D^0 and \bar{D}^0 samples prefer a large negative interference term when the phase space is restricted to suppress DCS contributions. By contrast, when the interference term is integrated over the entire Dalitz plot, it is found to be consistent with zero, with uncertainties comparable to those in this analysis. The variation of the interference effect in different phase-space regions motivates a detailed phase-space analysis of this mode in the future.

In summary, we find that the data are consistent with the no-mixing hypothesis at the 4.5% confidence level, and we set an upper limit $R_M < 0.054\%$ at the 95% confidence level. We measure the branching ratio for $D^0 \rightarrow K^+\pi^-\pi^0$ relative to $D^0 \rightarrow K^-\pi^+\pi^0$ to be $(0.214 \pm 0.008(\text{stat.}) \pm 0.008(\text{syst.}))\%$.

We are grateful for the excellent luminosity and machine conditions provided by our PEP-II colleagues, and for the substantial dedicated effort from the computing organizations that support *BABAR*. The collaborating institutions wish to thank SLAC for its support and kind hospitality. This work is supported by DOE and NSF (USA), NSERC (Canada), IHEP (China), CEA and CNRS-IN2P3 (France), BMBF and DFG (Germany), INFN (Italy), FOM (The Netherlands), NFR (Norway), MIST (Russia), MEC (Spain), and PPARC (United Kingdom). Individuals have received support from the Marie Curie EIF (European Union) and the A. P. Sloan Foundation.

many), INFN (Italy), FOM (The Netherlands), NFR (Norway), MIST (Russia), MEC (Spain), and PPARC (United Kingdom). Individuals have received support from the Marie Curie EIF (European Union) and the A. P. Sloan Foundation.

* Also at Laboratoire de Physique Corpusculaire, Clermont-Ferrand, France

† Also with Università di Perugia, Dipartimento di Fisica, Perugia, Italy

‡ Also with Università della Basilicata, Potenza, Italy

- [1] L. Wolfenstein, Phys. Lett. B **164**, 170 (1985); J. F. Donoghue, E. Golowich, B. R. Holstein and J. Trampetic, Phys. Rev. D **33**, 179 (1986); A. F. Falk, Y. Grossman, Z. Ligeti and A. A. Petrov, Phys. Rev. D **65**, 054034 (2002); G. Burdman and I. Shipsey, Ann. Rev. Nucl. Part. Sci. **53**, 431 (2003); A. F. Falk, Y. Grossman, Z. Ligeti, Y. Nir and A. A. Petrov, Phys. Rev. D **69**, 114021 (2004).
- [2] Belle Collaboration, L. M. Zhang *et al.*, Phys. Rev. Lett. **96**, 151801 (2006).
- [3] Unless otherwise stated, particle types and decay processes imply also their charge conjugates.
- [4] CLEO Collaboration, S. Kopp *et al.*, Phys. Rev. D **63**, 092001 (2001).
- [5] G. Blaylock, A. Seiden and Y. Nir, Phys. Lett. B **355**, 555 (1995).
- [6] BABAR Collaboration, B. Aubert *et al.*, Nucl. Instrum. Meth. A **479**, 1 (2002).
- [7] BABAR Collaboration, B. Aubert *et al.*, Phys. Rev. Lett. **91**, 121801 (2003); BABAR Collaboration, B. Aubert *et al.*, Phys. Rev. Lett. **91**, 171801 (2003).
- [8] W. D. Hulsbergen, Nucl. Instrum. Meth. A **552**, 566 (2005).
- [9] Particle Data Group, W.-M. Yao *et al.*, J. Phys. G **33**, 1 (2006).
- [10] CLEO Collaboration, G. Brandenburg *et al.*, Phys. Rev. Lett. **87**, 071802 (2001); Belle Collaboration, X. C. Tian *et al.*, Phys. Rev. Lett. **95**, 231801 (2005).
- [11] M. Pivk and F. R. Le Diberder, Nucl. Instrum. Meth. A **555**, 356 (2005).
- [12] P. E. Condon and P. L. Cowell, Phys. Rev. D **9**, 2558 (1974).